Article
DOI: 10.1002/bkcs.12271 J. Kim et al. BULLETIN OF THE KOREAN CHEMICAL SOCIETY

Design, Synthesis, and Biological Evaluation of Imidazopyrazinone Derivatives as Antagonists of Inhibitor of Apoptosis Proteins (IAPs)

Jisook Kim,[†] **Inhwan Bae**,[‡,§] **Jiyoung Song**,[‡] **Younghoon Kim**,[‡] **Younggil Ahn**,[‡] **Hyun-Ju Park**,[†] **Ha Hyung Kim**,[¶,*] **and Dae Kyong Kim**[§,*]

[†]*School of Pharmacy, Sungkyunkwan University, Suwon 16419, Republic of Korea*
[‡]*Hanmi Research Center, Hanmi Pharm. Co. Ltd., Gyeonggi-Do 18469, Republic of Korea*
[§]*Department of Environmental and Health Chemistry, College of Pharmacy, Chung-Ang University, Seoul 06974, Republic of Korea. *E-mail: kimdk@cau.ac.kr*
[¶]*Biotherapeutics and Glycomics Laboratory, College of Pharmacy, Chung-Ang University, Seoul 06974, Republic of Korea. *E-mail: hahyung@cau.ac.kr*
Received November 18, 2020, Accepted March 8, 2021

Apoptosis inhibitor (IAP) proteins are overexpressed in many cancers and implicated in tumor growth, so the development of antagonist that disrupts with the binding of IAP to their partner protein is a promising therapeutic strategy. In an effort to increase cellular activity and improve favorable drug-like properties, we newly designed and synthesized monovalent analogues based on imidazopyrazinone structure of **9**. Optimization of cellular potency led to the identification of **17**, which showed increase of submicromolar activity (GI_{50} = 234 nM) and caspase-3 activation (6.3-fold) in MDA-MB-231 breast cancer cells. These findings clearly show the potential for **17** as a promising monovalent antagonist for the development of an effective anticancer treatment.

Keywords: Imidazopyrazinone, Inhibitors of apoptosis proteins antagonist, Second mitochondrial activator of caspases, Apoptosis

Introduction

Programmed cell death or apoptosis is closely related to inhibitory of apoptosis protein (IAP) and regulates cell death. These apoptosis inhibiting proteins are known as proteins involved in the regulation of various signaling pathways. Some of the baculovirus inhibitor of apoptosis protein repeat (BIR) domains of IAP bind to caspases, which are proteases that induce and regulate apoptosis of cells, thereby inhibiting cell death.[1,2] In addition, it has been revealed that inhibitory of apoptosis protein plays an additional role in addition to the negative feedback of apoptosis, including cell differentiation, cell motility, migration, invasion, and metastasis.[3–6] Therefore, the development of new IAP antagonists can serve the potential of new therapeutic options, and can provide an opportunity to increase clinical efficacy and resolve refractory and resistance causes through combination therapy with approval agents.[7–9]

Through the previous study of the structure of the second mitochondrial activator of caspases (SMAC) protein that induces apoptosis mechanism *in vivo*, various studies on the natural IAP-binding amino acid sequence that can bind to the BIR3 and BIR2 domains of IAP have been conducted. Based on the results of research on the binding structure of SMAC and BIR domains, it was found that the key amino acid sequence of SMAC participating in the binding interaction is Ala(P1)-Val(P2)-Pro(P3)-Ile (P4) tetramer, **1**, and the variety of modified monovalent antagonists have been developed.

The development of an IAP antagonists, called a monomers or monovalents, are based on the Amgen-IAP, **2** published in 2004 by Amgen's research group and the structure of Novartis' LBW242, **3** announced in 2007 (Figure 1).[10,11] The key sequence, Ala-Val-Pro-Ile (AVPI) had no cell permeability, therefore, Amgen-IAP, **2** with modification of Ile(P4), and LBW242, **3** through cyclization between Pro(P3) and Ile(P4) developed as the IAP antagonists with cellular activities. However, these antagonists have an unmet need for new IAP antagonists with improved activity due to low cellular activity. In this paper, we investigated the structure–activity relationship of a novel imidazopyrazinone-based derivatives and characterized its pharmacokinetics and pharmacodynamics as a potent SMAC mimetics.

Experimental

General Information. Reagents and solvents were purchased from commercial sources and were used without purification. Reactions were monitored by thin-layer chromatography. All purifications were proceed flash chromatography system (ISCO, combiflash Rf^+; Lincoln, NE, USA). ^{1}H NMR and ^{13}C NMR spectra were recorded on

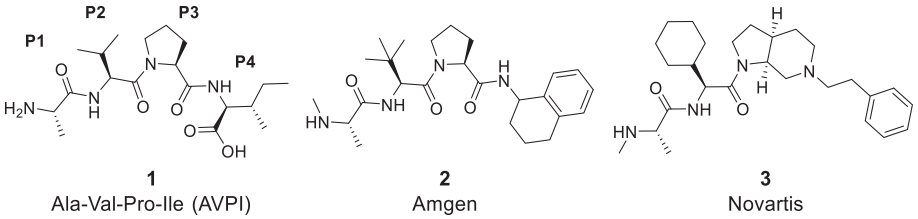

Figure 1. Structures of AVPI and monovalent IAP antagonists.

Bruker, Avance DPX 300 (300 MHz for ^{1}H, 75 MHz for ^{13}C; Seattle, WA, USA). Mass spectra were obtained on Waters Aquity UPLC/QTOF. High-performance liquid chromatography was used Agilent, 1200 series using a Gemini-NX C18 4.6 × 150 mm, 3 μm column eluting with a mixture of acetonitrile and Methanol (80:20 [vol/vol %]) containing pH 7.0 buffer (25 mM Na_2HPO_4, pH 7.0 with H_3PO_4) with a 15 min gradient of 55–40% and Phenomenex Kinetex C18, 4.6 × 100 mm, 2.6 μm column eluting with a mixture of acetonitrile and Methanol (80:20 [vol/vol %]) containing pH 7.5 buffer (50 mM ammonium formate, pH 7.5 with ammonia) with a 20 min gradient of 55–15%. Liquid chromatography–mass spectrometry results were obtained on Waters QTOF (SYNAPT G2) with electrospray ionization.

Cell Growth Inhibition Assay. MDA-MB-231 breast cancer cells (ATCC # HTB-26) were plated in 96-well plates at a density of 1.0×10^4 to 1.5×10^4 cells/well. After 24 h, the cells were treated with test compounds at a concentration of 0 μM, 0.5 μM, l μM, and 5 μM, respectively, for 12 h to caspase 3/7 and for 24 h to caspase 9. Then, media were removed and the cells were washed two times with phosphate-buffered saline at 4 °C. The half maximal growth inhibition concentration (GI_{50}) was determined using GraphPad Prism (GraphPad Software; San Diego, CA, USA).

BIR3 Binding Affinity Assay. X-chromosome-linked inhibitors of apoptosis proteins (XIAP) baculovirus inhibitors of apoptosis proteins repeat (BIR) prediluted by 1.25 μM was placed into a black, round-bottom 96-well plate at 5 μL/well, and 4F (AbuRPF-K(5-Fam)-NH_2) prediluted by 0.0625 μM was added thereto at 10 μL/well under a dark condition. At the time, XIAP BIR is a 241–356th amino acid residue of human XIAP protein, which was prepared by transforming *Escherichia coli* BL21(DE3) cells with a recombinant vector prepared from pET28a vector (Novagen) using standard DNA cloning process and polymerase chain reaction (PCR) method (see Sambrook & Russell, Molecular cloning, Chapter 1. Third edition).

Caspase Activation Assay. The cells were treated with a solution of the analysis samples and media (1:1) in an amount of l00 μL/well using Caspase-Glo™ 3/7 Assay Kit (Cat#. 08090; Promega, USA). After the cells were incubated at 37 °C for 2 h, luminescence was measured using Infinite™ M1000 multireader (Tecan).

Animal Studies. The Sprague-Dawley rat (SD rat) received imidazopyrazinone derivatives either by intravenous (iv) injection (1 mg/kg) in the tail vein, or by oral (po) administration (3 mg/kg). The pharmacokinetic parameters (area under curve $(AUC)_{0-24}$, AUC_{inf}, and half-life) of imidazopyrazinone derivatives were calculated by noncompartment assay via WinNonLin® (Certara, NJ, USA). C_{max} and T_{max} were obtained directly from the observed data. Bioavailability (BA) was calculated as follows: BA (%) = $(AUC_{0-24\ po} \times Dose_{iv})/(AUC_{0-24\ iv} \times Dose_{po}) \times 100$.

The SD male rat (8 weeks age, n = 3/group) were obtained from the Koatech, Inc. (Pyeongtaek, Korea). The experimental processes on animals, and animals care were carried out in accordance to study protocol approved by the Hanmi Research Center Institutional Animal Care and Use Committee as Animal Ethics Committee.

Results and Discussion

Previously reported LBW242, **3** derives a new 5–6 membered bicyclic template by changing AVPI's Proline and Isoleucine cyclization and Valine to cyclohexylglycine (Chg). However, LBW242, **3** exhibits moderate binding

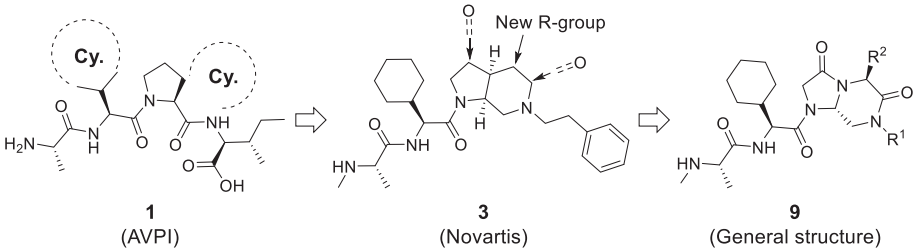

Figure 2. General design method of compound **9**.

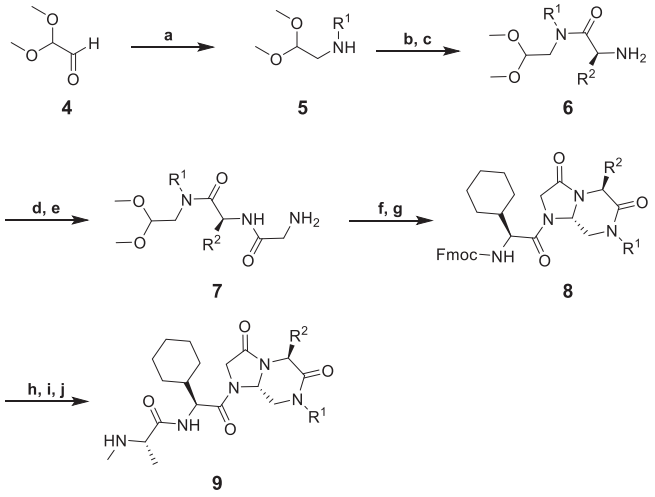

Scheme 1. Synthesis of the general compound **9**. Reagents and conditions: (a) R^1-NH_2, $NaCNBH_3$, MeOH, rt., 12 h; (b) Fmoc-amino acid, HATU, DIPEA, DCM, rt., 4 h; (c) 10% piperidine/DCM, rt., 2 h; (d) Fmoc-Gly-OH, EDCI, HOBT, DIPEA, DCM, rt., 12 h; (e) 10% piperidine/DCM, rt., 2 h; (f) Fmoc-Chg-OH, EDCI, HOBT, DIPEA, DCM, rt., 4 h; (g) formic acid, 80 °C, 3 h; (h) 10% piperidine/DCM, rt., 2 h; (i) Boc-MeAla-OH, EDCI, HOBT, DIPEA, DCM, rt., 4 h; (j) 4 M HCl/dioxane, rt., 2 h.

affinity, and peptides like this have a common drawback, that is, poor cell permeability, similar to other peptidic compounds. Therefore, extensive modifications using reduction or insertion of other binding partner were carried out to propose potent and cell-permeable peptidomimetics. In order to improve cellular activity, we designed a new derivative **9** with the insertion of the carbonyl groups in LBW242 to reduce flexibility and to introduce a new R. Most monovalent structures induce an "opposite U-shaped" binding conformation, which bind to the IAP BIR3 domain through its hydrophobic interaction with Trp323. Additionally, the structure of the R^2-introduced compounds was designed as an "opposite Y-shaped" binding conformation to have π-π stacking interaction with Tyr324 to improve binding affinity (Figure 2).

The general synthetic procedure for the preparation of structure **9** is shown in Scheme 1. Commercially available dimethylacet aldehyde, **4** was coupled with R^1-NH_2 via reductive amination to give **5** with a good yield. The secondary amine **5** was coupled to unnatural amino acid with R^2-group using 1-[Bis(dimethylamino)methylene]-1H-1,2,3-triazolo[4,5-b]pyridinium 3-oxid hexafluorophosphate (HATU) amide coupling reaction, which, after Fmoc-deprotection with piperidine, yielded **6**. The **7** was obtained through coupling and deprotection in the same way as Fmoc-Gly-OH. The primary amine **7** was coupled to Fmoc-Chg-OH, which, after cyclized with formic acid using sealed tube gave **8**. At this time, it should be noted that if the external reaction temperature exceeds 100 °C or less than 60 °C, undesirable compounds are obtained. The **8** was sequentially deprotected against Fmoc and coupled with Boc-MeAla-OH, followed by deprotection of Boc using 4 M HCl/Dioxane to yield **9**.

Table 1. Cell growth inhibitory activity of compounds **10–24** against MDA-MB-231 and Hs27 cell lines.

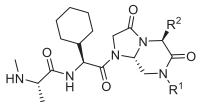

Cpd.	R^1	R^2	GI_{50} (nM)	
			MDA-MB-231	Hs27
2	-	-	276	>10 000
10	Benzyl	Benzyl	868	>10 000
11	Phenethyl	Benzyl	274	>10 000
12	Phenylpropyl	Benzyl	2758	>10 000
13	4-fluorophenthyl	Benzyl	657	>10 000
14	4-fluorophenthyl	4-methoxybenzyl	639	>10 000
15	Phenethyl	4-hydroxybenzyl	283	>10 000
16	Phenethyl	4-methoxybenzyl	1076	>10 000
17	Phenethyl	4-methylbenzyl	234	>10 000
18	Phenethyl	1H-indol-3-ylmethyl	818	>10 000
19	Phenethyl	Naphthalene-1-ylmethyl	379	>10 000
20	Phenethyl	Naphthalene-2-ylmethyl	170	>10 000
21	Benzyl	Naphthalene-2-ylmethyl	1940	>10 000
22	4-chlorobenzyl	Naphthalene-2-ylmethyl	2774	>10 000
23	4-methoxybenzyl	Naphthalene-2-ylmethyl	4584	>10 000
24	4-methoxyphenethyl	Naphthalene-2-ylmethyl	2008	>10 000

Table 2. Microsomal stability of **17** and **20**.

	Remaining % of parent molecule at 60 min		
Cpd.	Human	Dog	Rat
17	22	32	9
20	24	46	25

Table 3. *In vitro* evaluation of **17** and **20** in various CYP isozymes.

	CYP isozymes (IC_{50}, μM)				
Cpd.	1A2	2C9	2C19	2D6	3A4
P.C.[a]	2.29	42.18	>50.0	>50.0	<0.0062
17	>50.0	42.18	>50.0	>50.0	<0.62
20	39.38	19.68	23.78	36.82	<0.62

[a] P.C., positive control; Furafylline (1A2), sulfaphenazole (2C9), tranylcypromine (2C19), Qunidine (2D6), Ketoconazole (3A4).

This privileged structure **9** was analyzed by solution-phase 2D-NMR spectroscopy (^{1}H-^{1}H COESY and ^{1}H-^{1}H NOESY) to conform on accurate structure of 5–6 bicyclic template and chirality of junction proton.[12] Compounds **10**–**23** were prepared according to the same synthetic route as Scheme 1. More detailed synthetic methods and conditions of representative compound **17** are shown in Supporting Information.

We newly designed and synthesized monovalent IAP antagonists based on imidazopyrazinone, and these compounds were assessed for MDA-MB-231 breast cancer cells and Hs27 foreskin normal cells. All of compounds **10**–**24** did not show cellular activities with more than >10 000 nM to Hs27 (Table 1

). In addition, **3** as reference compound showed the cellular activity of over 10 000 nM against MDA-MB-231. In order to determine the optimized chain length of R^1, the cell growth inhibition of compounds **10**–**12**, which the simplest R^2 is benzyl, were compared. As a result of comparison using **2** as a control material, **11** into which a phenethyl group was introduced showed the most similar activity. In order to confirm the binding ability of the active compounds to XIAP-BIR3 was compared, BIR3 binding affinity assay was performed to obtain *Ki* values of 315 and 356 nM for compound **2** and compound **11**, respectively.

These increased activities were thought to have various interactions with Trp323 or Tyr324 of the BIR3 domain by the introduction of the R^2 group. In order to identify other substituents of phenethyl length, **13** and **14** having 4-fluorophenthyl were tested, but lower cell line activity than **11** was confirmed. The phenethyl was fixed on R^1-position, and various substituents for R^2 were evaluated. As a result of comparing compounds **15**–**20**, it was possible to confirm **17** (GI_{50} = 234 nM) and **20** (GI_{50} = 170 nM), which are more potential than **11** (GI_{50} = 274 nM). Therefore, naphthalene-2-ylmethyl, which is R^2, which has the best activity, was immobilized and compounds **21**–**24** in which R^1 was substituted were tested. However, all of these compounds **21**–**24** showed cellular activity of more than 1000 nM. Therefore, among these compounds, sequential evaluation was performed on **17** and **20**. To derive lead compound, **17** and **20** having good cellular activity were tested in microsomal stability and CYP isozyme. Both compounds **17** and **20** showed moderate microsomal stability as the lead compound criteria (Table 2).

In CYP inhibition assay, 17 showed strong inhibition of CYP3A4 and weak four major CYP isozymes, whereas **20** strongly inhibited CYP3A4 and moderate two major CYP isozymes (Table 3). These results indicate that **17** has a lower risk of drug–drug interactions than **20**, although both showed strong inhibition of 3A4.

According to similar CYP inhibition and microsomal stability results, caspase-3 activation assay was performed in MDA-MB-231 cells with 1 μM concentration of compounds to select lead compound. As results of the assay, **2** increased 5.6-fold activity compared to the control group, whereas compounds **17** and **20** increased 6.3-fold and 3.8-fold, respectively. Therefore, **17** was nominated as the lead compound for developing compound and the following evaluation was conducted.

We subsequently conducted an *in vivo* pharmacokinetic study using the SD rat model (Table 4). Oral administration of 3 mg/kg dose was found that the absolute bioavailability was 1.8% after oral administration, while the values of AUC_{0-24}, C_{max}, and half-life were 10.0 ng h/mL, 1.7 ng/mL, and 56.6 h, respectively. Following 1 mg/kg iv dose of **17**, Clearance (Cl) was 5.2 mL/min/

Table 4. Pharmacokinetic parameters of compound **17** following a single intravenous (1 mg/kg) or oral (3 mg/kg) administration in SD rat (n = 3).

Route	Dose[a] (mg/kg)	AUC_{0-24} (ng h/mL)	C_0 (ng/mL)	C_{max} (ng/mL)	T_{max} (h)	$t_{1/2}$ (h)	V_d (L/kg)	Cl (L/h*kg)	BA (%)
iv.	1	189.2 ± 14.2	473.3 ± 39.0	-	-	8.6 ± 0.5	64.6 ± 8.7	5.2 ± 0.4	-
po.	3	10.0 ± 3.2	-	1.7 ± 0.8	2.0 ± 0.0	56.6 ± 53.7	3114 ± 2078	141.7 ± 109.0	1.8

[a] As amount of free form.

kg, the $t_{1/2}$ was 8.6 h, and the volume of distribution (V_d) was 64.6 L/kg. Altogether, our results showed that **17** presented moderate clearance and high distribution rates in SD rat by iv dosing. Therefore, it is necessary to investigate whether the dosing regimen is iv bolus or iv infusion depending on the convenience of administration with combination therapy.

Conclusion

In summary, we developed a synthesis of a novel series of SMAC mimetics using a imidazopyrazinone-based structure. We found that introducing these derivatives provide dramatically improved cellular potency with submircomolar activities, compared to **2** and **3**. In these results of imidazopyrazinone derivative, it was thought that the introduction of the R^2 group induced various interactions with Trp323 or Tyr324 of the BIR3 domain, thereby having higher activity. The imidazopyrazinone scaffold showed good caspase activation at low concentration and a remarkable cellular potency. More detailed and dose-dependent studies on pharmacokinetics, absorption, distribution, metabolism and elimination, efficacy, and toxicity of **17** will be explored in the future.

Acknowledgments. We are grateful to J.Y. Byun and T.H. Song for useful discussions and critical reading of the manuscript. We thank the Pharmacology Team at Hanmi Research Center for cell line screening and evaluation of pharmacokinetics studies.

Conflict of Interest. The authors declare no conflicts of interest.

Supporting Information. Additional supporting information may be found online in the Supporting Information section at the end of the article.

References

1. S. Fulda, D. Vucic, *Nat. Rev. Drug Discov.* **2012**, *11*, 109.
2. F. Cossu, M. Milani, *Comput. Struct. Biotechnol. J.* **2019**, *17*, 142.
3. R. Lau, M. A. C. Pratt, *ISRN Oncol.* **2012**, *2012*, 928120.
4. K. Geddes, J. G. Magalhaes, S. E. Girardin, *Nat. Rev. Drug Discov.* **2009**, *8*, 465.
5. J. Silke, P. Meier, *Cold Spring Harb. Perspect. Biol.* **2013**, *5*, a008730.
6. J. Berthelet, L. Dubrez, *Cell* **2013**, *2*, 163.
7. H. Cong, L. Xu, *J. Med. Chem.* **2019**, *62*, 5750.
8. J. B. Jaquith, *Pharm. Pat. Anal.* **2014**, *3*, 297.
9. R. Ali, S. Singh, *Curr. Med. Chem.* **2018**, *25*, 3768.
10. T. K. Oost, C. Sun, R. C. Armstrong, A. Al-Assaad, S. F. Betz, L. Thomas, T. L. Deckwerth, H. Ding, S. W. Elmore, R. P. Meadows, E. T. Olejniczak, A. Oleksijew, T. Oltersdorf, S. H. Rosenberg, A. R. Shoemaker, K. J. Tomaselli, H. Zou, S. W. Fesik, *J. Med. Chem.* **2004**, *47*, 4417.
11. D. Chauhan, P. Neri, M. Velankar, K. Podar, T. Hideshima, M. Fulciniti, P. Tassone, N. Raje, C. Mitsiades, N. Mitsiades, P. Richardson, L. Zawel, M. Tran, N. Munshi, K. C. Anderson, *Blood* **2006**, *109*, 1220.
12. G. Eschenburg, A. Eggert, *Cancer Res.* **2012**, *72*, 2645.

